Received: 15 February 2019 | Revised: 26 March 2019 | Accepted: 5 April 2019

DOI: 10.1002/bit.26987

ARTICLE

WILEY BIOTECHNOLOGY BIOENGINEERING

EWOD silicon biosensor for multiple nucleic acids analysis

Salvatore Petralia[1] | Daniele Motta[2] | Sabrina Conoci[1]

[1]STMicroelectronics, Stradale primosole, Catania,

[2]Distretto Tecnologico Sicilia Micro e Nano Sistemi, VIII Strada, 5-Zona Industriale, Catania, Italy

Correspondence
Salvatore Petralia and Sabrina Conoci, STMicroelectronics, Stradale primosole, Catania.
Email: salvatore.petralia@st.com; sabrina.conoci@st.com

Funding information
Italian MIUR, Grant/Award Number: This work was supported by MIUR by means of the na

Abstract

In this paper, a miniaturized biosensor containing 96 silicon microchambers electroloaded with nano-volumes of liquid (EW-chip) is presented. The liquid electroloading is achieved by the appropriate modulation of interface properties. The surface chemistries have been studied to guarantee effective interface properties for both electrowetting on dielectric actuation and biocompatibility versus biochemical reactions. The silicon microchambers are 200 nl in volume and are connected to a specific system of electrodes able to deliver liquid sample on each well. The device also integrates temperature sensors and heaters to perform biochemical reactions. On that, the effectiveness of this device has been successfully proven towards the nucleic acids detection via real-time polymerase chain reaction amplification. Hepatitis B virus genome target has been used to assess the device performance. Results show very uniform amplification over the 96 microchambers without any cross-contamination process. These features make this system a very appealing potential solution for genetic point-of-care devices where a high level of parallelism of analysis is required.

KEYWORDS
bionsensor, EWOD, microchip, nucleic acids, silicon

1 | INTRODUCTION

The development of miniaturized microfluidic systems for multiple analysis involving small sample volume is very attractive for a broad range of biosensor applications, including the detection of nucleic acids (Battaglia, Petralia, Vicario, Cirillo, & Conoci, 2019; Mark, Haeberle, Roth, von Stettenz, & Zengerlez, 2010; Petralia, Castagna, Motta, & Conoci, 2016), proteins (He & Herr, 2010; Petralia, Ventimiglia, Ceschia, Gasparin, & Verardo, 2017), and environmental analyses (Casilli et al., 2004; Giancane, Borovkov, Inoue, Conoci, & Valli, 2013; Italiano et al., 2009; Rella et al., 2000; C. Zhao, Ge, & Yang, 2017). Among these applications, in the last decades great attention has been received by the detection of nucleic acids in miniaturized biochip (Lab-on-Chip [LoC]) devices (Callari, Petralia, Conoci, & Sortino, 2008; Liu et al., 2018; Petralia, Sciuto, & Conoci, 2017; Sortino, Petralia, Condorelli, Conoci, & Condorelli, 2003). This is mainly driven by the relevant impact that both miniaturization and portability have in several applicative fields such as infectious diseases, gene expressions, single-nucleotide polymorphism, environmental testing, food control, and forensic science (Pollack, Fair, & Shenderov, 2000), where crucial requirements such as fast response (few hours), easy to use, portability, good sensitivity (up to 10 copies/reaction), and multiplexing of analysis (viz., the aptitude to detect many pathogens in a single run) are required.

In this context, miniaturized biochips with multiple microreactors are very appealing for applicative use since they enable an increased level of parallelism of analysis allowing analytical procedures to be conducted simultaneously on a single biological sample. In this view, silicon technologies such as very large system integration (VLSI) and microelectrical-mechanical systems (MEMS) offers many advantages for the fabrication of miniaturized LoC, especially if combined with plastic materials. In fact, the silicon–plastic hybrid technologies allow the possibility to combine multiple functions such as fluidic and thermal management, integration of optical and electrical transduction methods with microelectronics circuit ("intelligence on board") (Jang et al., 2011; Libertino, Conoci, Scandurra & Spinella, 2013).

Additionally, they can leverage on consolidated production technologies and industrialization processes.

In miniaturized multichambers biochips, a crucial point is the manipulation of a small volume of liquid. This handling is difficult to be managed and very complex microfluidic systems are necessary (Petralia and Conoci, 2017). These systems must assure the driving of the liquid in the final location preventing air bubbles entrapment during the sample liquid loading that should create negative consequence in the final results of the analysis. Actually, the presence of bubbles is very deleterious since important process parameters, such as reaction volume, equilibrium of the reagents, pressure, and temperature, are adversely affected by them.

In this view, among the several methods to manipulate a small amount of liquid not involving complex microfluidic systems, electrowetting on dielectric (EWOD) represents one of the most intriguing approaches. It offers the possibility to move a small volume of fluids by means of electrical actuation and, additionally, offer the advantages to be easily integrated into a miniaturized device (Nelson & Kim, 2012). EWOD is a physical phenomenon whereby an electric field generated by a voltage potential is able to change the interfacial tension between liquid and insulator dielectric surfaces. This electrostatic effect charges the electrical double layer and induces a wettability change at dielectric/liquid interface. This effect is well described by the Lippman-Young equation, where the contact angle formed at the interface is correlated to the value of the applied voltage and to the physical parameters of the dielectric material, such as the dielectric constant and thickness (Mugele & Baret, 2005; Y.-P. Zhao & Wang, 2013).

The EWOD phenomenon is largely influenced by the surface chemistry. In fact, the integration of a suitable coating surface is a critical process for microfluidics effectiveness. In this context, many surface chemistry strategies have been proposed in the literature. Since the early 1990s, Sondag-Huethorst et al. showed how to modulate the charging of the electrical double layer by appropriate surface molecular layers (Sondag-Huethorst & Fokkink, 1994a) or redox molecules immobilized at the dielectric/liquid interface (Sondag-Huethorst & Fokkink, 1994b). Hydrophilic layer of polyvinyl alcohol has been also used to improve droplet manipulation (Trantidou, Elani, Parsons, & Ces, 2017). Thanks to these features, the method has been successfully used in several technological applications mainly including adjustable lenses (Berge & Peseux, 2000), reflective displays (Hayes & Feenstra, 2003) and microfluidic applications based on droplet actuation (Marziliano et al., 2015).

In this paper, an effective EWOD fluidic actuation of nano-volumes of liquid in a silicon biosensor composed of 96 microchambers is achieved by appropriate modulation of interface properties. Various chemical coating layers were investigated to create proper surface conditions for an effective EWOD effect. The change of surface properties was evaluated at different voltage application by static contact angle measurements. Finally, the ability to detect genetic target consisting in the hepatitis B virus (HBV) genome was assessed by real-time polymerase chain reaction (RT-PCR), achieving innovative solutions for multiparallel detection of biotargets in a single biochip. This can be very useful for many diagnostic sectors, especially when fast response, good sensitivity, and multiplexing of analysis are crucial aspects for the applicative use. In particular potential applications of this system should be in healthcare area for the detection of bacterial species for sepsis disease (Chun et al., 2015) and in food control sector for the detection of pathogens such as *Legionella pneumophila* and Salmonella where sensitivities of 10,000 and 100,000 CFU/ml are requested, respectively (Poltronieri, Mezzolla, Primiceri & Maruccio, 2014).

2 | EXPERIMENTAL DETAILS

2.1 | Chemicals and materials

The 3-glycidoxypropyltrimethoxysilane (GOPS), ethanolamine, and ethilendiamine were purchased by Sigma-Aldrich (Saint Louis, MI). The bovine serum albumin fraction V (BSA) has been purchased from Euroclone (Milan, Italy), while the additives sodium dodecyl sulfate, sodium chloride, and sodium citrate were purchased by Sigma-Aldrich. All reagents were used as received.

All reagents for the HBV RT-PCR experiments were purchased from Clonit (kit ref. product CLO-FO2 HBV MMIX KIT 48) and used according to the instruction for use. The target used was the hepatitis B virus (HBV) clone (ref. product CLO-05960116 HBVComplete Genome). RT-PCR experiments were performed using a Master Mix solution (volume 10 μl) containing clonit buffer (× 1) and Taq DNA polymerase, 0.5 μM of PCR primers.

The indium tin oxide (ITO) coated PET electrode (surface resistivity 100 Ω/sq and thickness 5 mil) was purchased by Sigma-Aldrich.

2.2 | EW-chip

The EW-chip was manufactured by silicon–plastic hybrid technology (Figure 1). The silicon part consists of a microchip of size 1.7 cm x 1.2 cm (thickness of about 1 mm) manufactured by standard VLSI technology. The manufacturing process started by a silicon wafer with the following steps involving SiO_2 thermal deposition (4,000 Å), AlCu deposition (1,000 Å), lithography followed by etching to create the metal strips. After that, a tetraethylorthosilicate (TEOS) deposition (8,000 Å) was carried out followed by lithography and etching for open the contact with the metal strips. The wafer was then taped and trench lithography carried out to create the microchambers. After resist removal, 8,000 Å of TEOS were then deposed. At the end of this manufacturing process, the bottom part containing integrated temperature sensors and heaters made of metal strips in AlCu (strips size is 4.0 ± 0.1 μm spaced with a distance of 5.0 ± 0.1 μm for the temperature sensor and 115.0 ± 0.1 μm spaced with a distance of 30.0 ± 0.1 μm for the heater). The top part contains in 96 silicon microchambers squared shaped (800 × 800 × 400 μm) with a pitch of 500 μm (microchamber volume 200 nl).

The polycarbonate ring (1.7 cm × 1.2 cm × 2.5 mm) was designed to contain a total volume of liquid of 20 ul. The ring was sonicated for

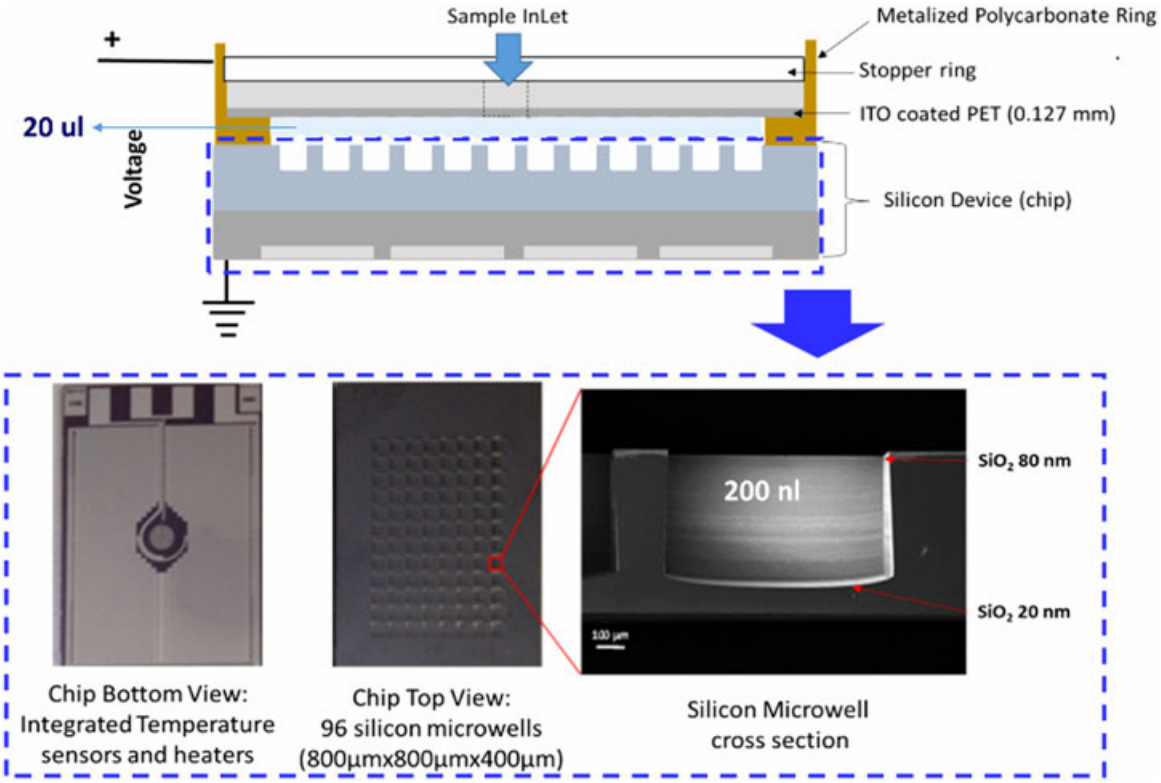

FIGURE 1 EW-chip structure [Color figure can be viewed at wileyonlinelibrary.com]

60 s in a water bath and glued on the silicon device with silicon glue. After that, the ring was sputtered with gold by a cool sputtering system in argon gas (Emitech K650X Sputtering Coater, 180 s, 100 mA). After the sputtering process, the electrical conductivity of the ring was verified by an electrical tester. An ITO slide was placed at the top of the metalized plastic ring to work as an electrode for uniform voltage application. Finally, a polycarbonate stopper ring was placed over the ITO slide to stabilize the chip structure. An inlet of 1 mm in diameter was created into both the ITO slide and the stopper ring for the liquid loading.

The ITO slide was connected to a standard parameter analyzer that applies a sweep voltage from 0 to + 40 V for the fluidic electrical actuation by EWOD.

2.3 | X-ray photoelectron spectroscopy (XPS) measurements

XPS analysis was performed using a Kratos AXIS-HS spectrometer. The X-rays Mg-K1,2 with emission line at 1253.6 eV was used at the conditions of 10 mA and 15 keV with a pass energy of 40 eV. During the analysis, the residual pressure in the chamber was 10^{-7} Pa.

2.4 | Surface treatments and characterization

The chemical treatments (chemistry) used for the EW-chip have been the following.

2.4.1 | Chemistry—Plasma-O_2

EW-chip was treated with plasma-O_2 process by Sentech plasma generator (300 s, 100 W) with analytical grade oxygen gas.

At the end of the process, the surface was characterized by XPS analysis. The spectra (see Figure SI-1) show the diagnostic peaks for Si2p (30%), and O1s (56.5%). A lower peak for C1s (10.3%) was found due to the environmental contamination, a negligible peak for F1s (< 3%) probably due to the Si–O–F species.

2.4.2 | Chemistry—Epoxy-silane (GOPS)

EW-chip was first treated with plasma-O_2 process by Sentech plasma generator (300 s, 100 W) with analytical grade oxygen gas. Then a vapor phase silanization with GOPS was carried out in under vacuum oven (Binder), with the following conditions: 4 hr, 0.1 atm, 125°C. Finally, the device was dipped in a solution of ethylenediamine 50 mM in buffer phosphate (0.15 M at pH 9.2) for 4 hr at 55°C (Venticell oven). The devices were rinsed in deionized water and dried by nitrogen flow. All processes described above were performed in a clean room (class 1000).

The surface was then characterized by XPS analysis (see Figure SI-2) that show the diagnostic peaks of C1s (285.5 eV) and N1s (401.0 eV).

2.4.3 | Chemistry—Bovine serum albumin (BSA)

EW-chip was first treated with plasma-O_2 process by Sentech plasma generator (300 s, 100 W) with analytical grade oxygen gas. Then a vapor

phase silanization with GOPS was carried out in under vacuum oven (Binder), with the following conditions: 4 hr, 0.1 atm, 125°C. The final step was the deposition of BSA protein layer by dipping the device in BSA 1% aqueous solution, SSC ×2, SDS 0.1%, for 15 hr at 55°C (Venticell oven). The substrates were then rinsed in deionized water and dried by nitrogen flow. The protein layer was characterized by XPS analysis (data not showed), the spectra show the follow diagnostic peaks: C1s at 285 eV (17.31%), O1s (53.70), N1s at 400 eV (2.46%) and Si2p (24.77%). The diagnostic peak for nitrogen (N1s) and the ratio C1s/Si2p value of about 0.7 confirm the presence of a protein layer.

2.4.4 | Chemistry—Ethanolamine

EW-chip was first treated with plasma-O_2 process by Sentech plasma generator (300 s, 100 W) with analytical grade oxygen gas. Then a vapor phase silanization with GOPS was carried out in under vacuum Oven (Binder), with the following conditions: 4 hr, 0.1 atm, 125°C. Finally, the device was dipped in a solution of ethanolamine 50 mM in buffer phosphate (0.15 M at pH 9.2) for 4 hr at 55°C (Venticell oven). The devices were rinsed in deionized water and dried by nitrogen flow. All processes described above were performed in a clean room (class 1000).

The XPS analysis (see Figure SI-3) for ethanolamine chemistry report the diagnostic peaks centered at 403.0 eV assigned to N1s (1.5%), the peak centered at 534.5 eV (51.4%) assigned to O1s and a double carbon peak centered to 286.8 eV (11%) for C1s. The deconvolution fit (Gaussian—30% Lorentzian) for the C1s peak, showing two main components assigned respectively to carbon linked to the electronegative species, C–O, and C–NH–R (286.8 eV) and assigned to C–C and C–H groups (285.0 eV).

2.4.5 | Chemistry—Ethylenediamine

EW-chip was first treated with plasma-O_2 process by Sentech plasma generator (300 s, 100 W) with analytical grade oxygen gas. Then a vapor phase silanization with GOPS was carried out in under vacuum oven (Binder), with the following conditions: 4 hr, 0.1 atm, 125°C. Finally, the device was dipped in a solution of ethylenediamine 50 mM in buffer phosphate (0.15 M at pH 9.2) for 4 hr at 55°C (Venticell oven). The devices were rinsed in deionized water and dried by nitrogen flow. All processes described above were performed in a clean room (class 1000).

The surface was characterized by XPS analysis. The spectrum (data not showed) in the range of 0–1000 eV reports the diagnostic peaks for Si2p (27%), O2p (51.6%), and C1s (10%). A Gaussian-Lorentz deconvolution for the C1s peak reports two main components: attributed to C–C and C–H carbon species and C–O species. The ratio C1s/Si2p value for the silanized surface is 0.37.

2.5 | EWOD—contact angle experiments

For the EWOD-contact angle measurements, a water drop volume of 1 µl was dispensed on the EW-chip surface by the dispensing apparatus of KRUSS contact angle meter and electroactuation (Karl Suss probe station) a voltage ranging from 0 to + 60 V, with a pulse time of 1 s and a pulse width of 0.5 s were applied by Semiconductor Parameter Analyser 4155C.

The obtained contact angle values after voltage application were measured by KRUSS contact angle meter.

2.6 | RT-PCR protocol

The RT-PCR experiments (see Section 2.7) were carried out using CLO-FO2 HBV kit purchased by Clonit containing a Master Mix solution including PCR buffer (× 1), Taq DNA polymerase, solution 0.5 µM of each forward (FW sequence GGT GAG TGA TTG GAG GTT) and reverse (Rev sequence CAA CAT CAG GAT TCC TAG) primers and standard HBV clone solutions. Positive sample was prepared by dissolving 5 µl of HBV clone (1×10^2 cps/µl) in 15 µM of Master Mix for a total volume of 20 µl. Negative samples were prepared by substituting the HBV clone with the same amount of water.

The PCR thermal program was: denaturation step 10 min at 95°C, followed by 45 cycles of 95°C for 15 s and 60°C for 60 s.

2.7 | EWOD–RT-PCR experiment

The EWOD–RT-PCR experiments were performed by the following steps.

2.7.1 | W-chip reagent preloading

A solution F/R primers were dispensed in the EW-chip microchambers by Perkin-Elmer (Waltham, MA) piezo microspotter to obtain a final concentration of 0.5 µM. After dispensing the chip was dried in an oven (Climacell).

2.7.2 | RT-PCR mix EWOD electroloading

Twenty microliters of the positive sample (see section 2.6) was pipetted through the EW-chip inlet at the device surface and a voltage ranging from 0 to + 40 V, with a pulse time of 1s and a pulse width of 0.5 s were applied by Semiconductor Parameter Analyser 4155C.

The chip was mounted into an appropriate holder and inserted into a portable thermal cycler (Q3-thermocycler developed by STMicroelectronic (Petralia, Sciuto, Di Pietr, et al., 2017) and thermally cycled according to the thermal program detailed in Section 2.6.

An RT-PCR amplification control experiment was executed by cycling the same mix (total volume of 20 µl) using Applied Biosystem 7500 Real-Time PCR equipment. Each experiment was replicated three times.

3 | RESULTS AND DISCUSSION

The EW-chip used in the present study is depicted in Figure 1. It is composed of a bottom silicon part and a top polycarbonate ring properly finished with a metal coating. The bottom silicon part

integrates temperature sensors and heaters for PCR thermal cycling, while the top part contains an array (8 × 12) of 96 squared microchambers of 200 nl in volume. The silicon chip was glued with a polycarbonate ring metalized with Au layer to obtain electrical contact. To guarantee the uniform voltage application in the EWOD experiments, a final ITO top-electrode was integrated into the top part of the device.

With the aim to be compatible with the typical PCR volume, the plastic ring was designed for obtaining a volume of 20 µl (total sampling volume of liquid) between the ITO electrode and the silicon chip.

A proper surface molecular coating was studied to achieve an appropriate hydrophobic surface avoiding spontaneously sample loading in absence of voltage application and switching to microfluidic loading only upon voltage application. Therefore, with the aim to study the influence of surface interface properties on for EWOD effect, the surface of SiO_2 layer (20 nm at the bottom surface and 80 nm in the walls), (see the cross- section reported in Figure 1) was modified with various surface chemistries: (A) plasma-O_2; (B) epoxy-silane; (C) BSA; (D) ethanolamine; (E) ethylenediamine (Figure 2). These treatments have been selected since they offer the possibility to obtain terminal chemical groups that are differently charged and, therefore, can create polarization/ionization effects at the surface upon potential application. This can differently modulate the surface wettability. Additionally, the (C)-(E) chemistries are known to be compatible with PCR processes (Petralia, Alessi, & Ventimiglia, 2012).

A first assessment of the surface wettability upon the chemical treatments above described was made by static CA measurements, directly taken at the silicon EW-chip surface (patterned with 96 microchambers). Table 1 summarizes the results. Data show that the most hydrophilic coating is the (A) (CA value 20°), while the other surface modifications (B–E) exhibit hydrophobic properties with CA values ranging between 97° and 110°. Note that all values are higher than those typically obtained for flat surfaces (Petralia, Castagna, Motta, & Conoci, 2016). This can be reasonably attributable to the patterning of the surface that induces an increase of the surface roughness.

The EWOD effect was first evaluated by applying various values of external voltage and measuring the CA values obtained, for all surface chemistries used. Figure 3 reports the static CA values versus the applied voltage between 0 and 60 V. The obtained data clearly

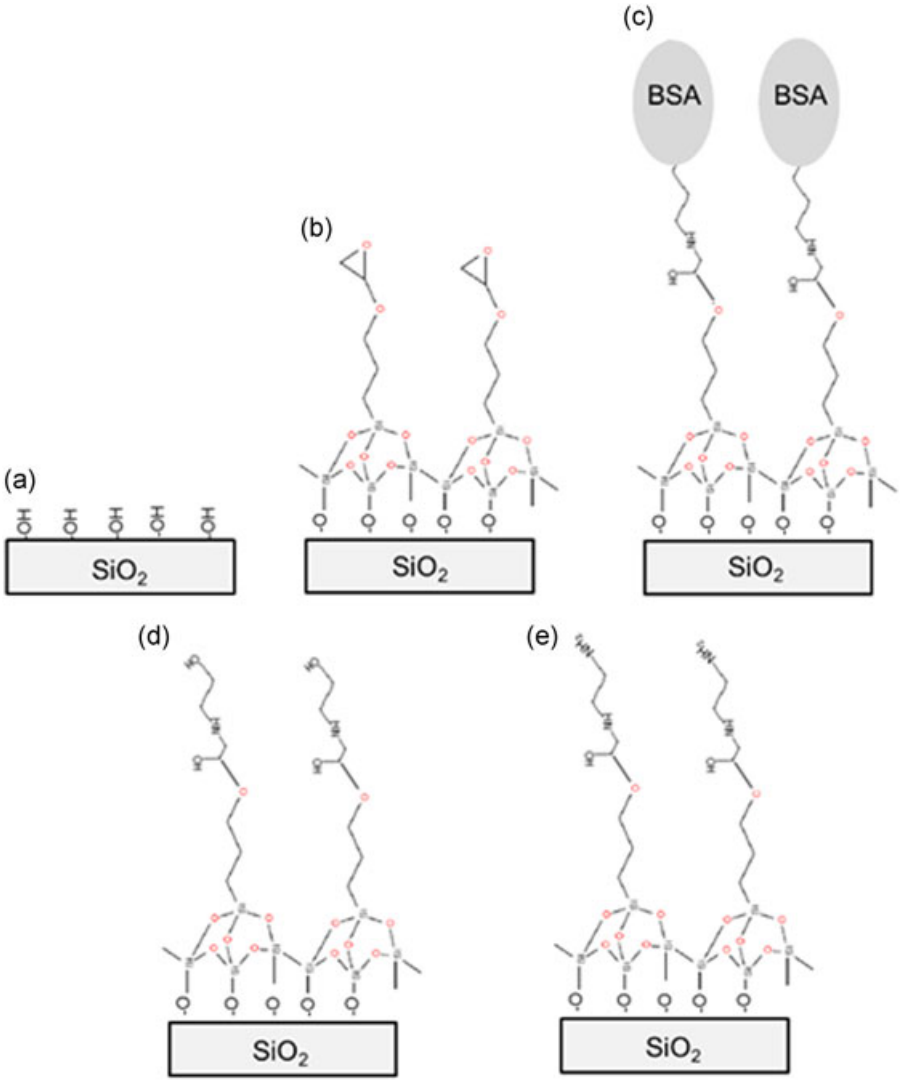

FIGURE 2 Surface chemistries: (A) plasma-O_2; (B) epoxy-silane; (C) bovine serum albumin (BSA); (D) ethanolamine; and (E) ethylenediamine [Color figure can be viewed at wileyonlinelibrary.com]

TABLE 1 Values of contact angles versus surface chemistries

Surface chemistry	Contact angle (deg.)
(A) Plasma-O_2	20 ± 5.3
(B) Epoxy-silane (GOPS)	100 ± 3.2
(C) Bovine serum albumine coating (BSA)	98 ± 3.5
(D) Ethanolamine coating	110 ± 3.2
(E) Ethylenediamine	97 ± 3.5

indicate an increase of surface hydrophilicity (lower CA value) with the increase of the external voltage application. In the case of procedure A (Plasma-O_2) this increasing slightly occurs since the starting surface was already quite hydrophilic.

Noteworthy, the surfaces terminated with an ionizable hydroxyl group (A and E chemistries) undergo a drastically increase of hydrophilicity upon voltage application according to the ionization of the uncharged hydroxyl group (–OH) forming many other oxidized silicon species (chemistry A) and negative charged hydroxyl ion (–O–) (chemistry B). On the contrary, the surfaces featured by amino and epoxy terminal groups (B and D chemistries), show a moderate change of wettability reaching CA values of about 30° and 50°, respectively. In the case of treatment C), despite the presence of multiple terminated chemical groups (due to the BSA protein), it exhibits a EWOD behavior similar to the B chemistry.

In our previous work Petralia et al. (2016) efficient EWOD effect was found for surface treated with C chemistry (exhibiting CA value less than 30°) upon external voltage application of 40 V. For this reason, this voltage value was then selected to be used for the microfluidic experiments actuated by EWOD effect. From Figure 3 it is possible to note that the wettability variation between 0 and 40 V in terms of CA values is 20° for chemistry A (CA value decreases from 20° to 0 °), 57° for chemistry B (CA value decreases from 97° to 40°), 38° for chemistry C (CA value decreases from 98° to 60°), 35° for chemistry D (CA value decreases from 100° to 65 °), 80° for chemistry E (CA value decreases from 110° to 30°), respectively. These findings clearly indicate that chemistry E exhibits the highest increase of wettability/hydrophilicity. This is in good agreement with surfaces terminated with hydroxyl groups, easy to be ionizable ($-OH \rightarrow -O^- + H^+$) forming charged terminal groups at the surface. A moderate increasing was found for chemistry B that presents surface terminated with less ionizable amino groups. Finally, C and D chemistries show a very moderate increase of wettability, while chemistry A exhibits the lowest increase due to the hydrophilic properties of the starting surface.

The next step of our study was focused on the assessment of the efficiency of microfluidic loading actuated by EWOD in EW-chip for all chemistries described. This was evaluated as the percentage of loaded microwells upon voltage application of 40 V using 20 μl of starting liquid sample. Results are reported in Figure 4.

It is noteworthy that the percentage of loaded microwells perfectly follows the increase of the surface wettability above discussed upon 40 V application. The EW-chip treated with E chemistry exhibiting the highest increase of surface wettability reaches 100% of loading. Similarly, the other B, C and D chemistries reach the lower amount of loaded wells of about 80%, 55%, and 40%, respectively, in agreement with their increasing values of surface wettability.

In the case of A chemistry due to the high starting hydrophilicity of the surface, a spontaneous fluidic loading was observed. Therefore, data for A chemistry were not included in Figure 4.

The final part of our study was devoted to demonstrate the use of EW-chip for multiple genetic analysis through RT-PCR amplification. The genetic assessment was carried out by using HBV clone as a biological target.

In view of the above results, we select the E chemistry as a chemical treatment for EW-chip that was previously loaded, in each microwell, with dried RT-PCR primer (forward and reverse) for the HBV amplification. A volume of 20 μl of RT-PCR master mix, containing

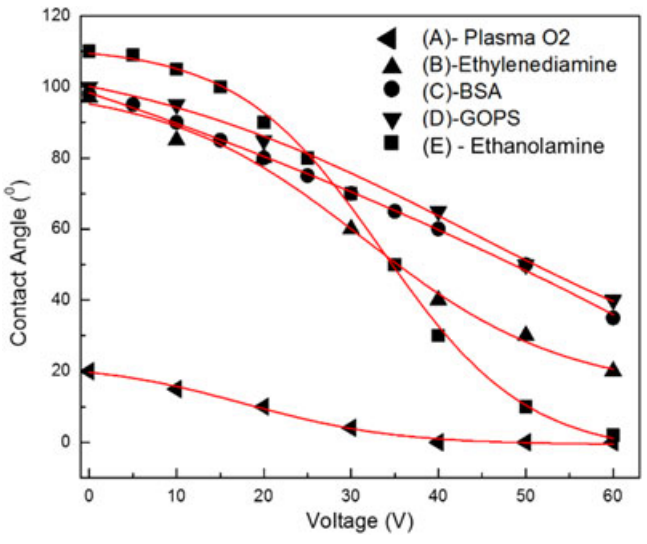

FIGURE 3 Contact angle values versus external voltage application for all surface chemistries. BSA: bovine serum albumin; GOPS: glycidoxypropyltrimethoxysilane [Color figure can be viewed at wileyonlinelibrary.com]

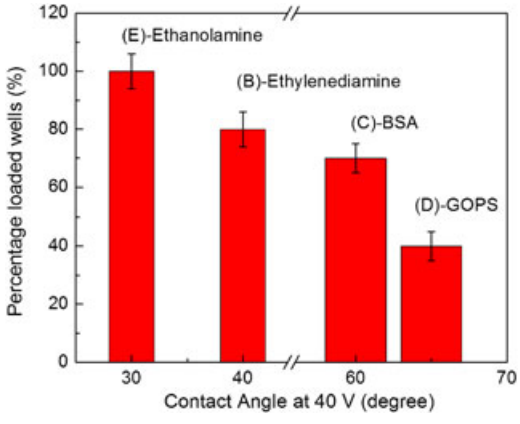

FIGURE 4 Percentage of loaded wells versus CA at 40 V for different surface chemistry. BSA: bovine serum albumin; GOPS: glycidoxypropyltrimethoxysilane [Color figure can be viewed at wileyonlinelibrary.com]

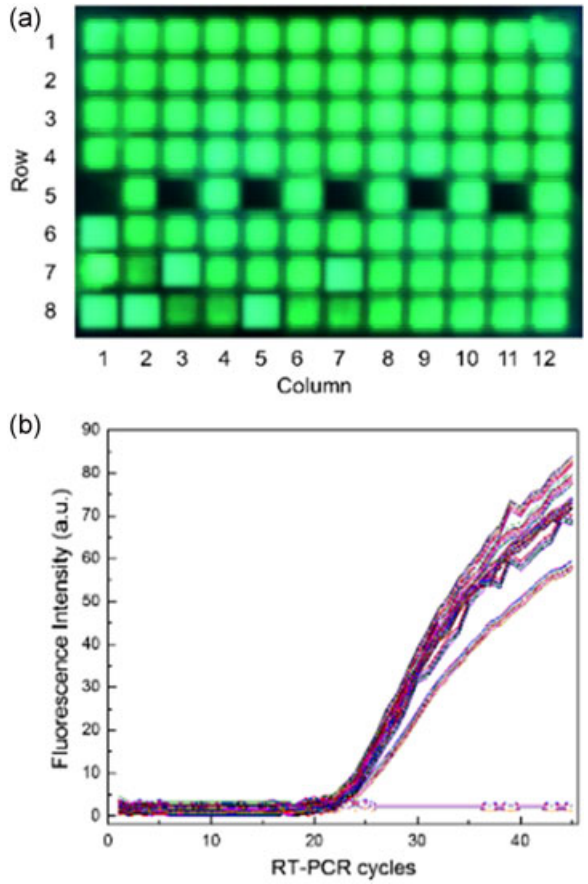

FIGURE 5 (a) Fluorescence image of 96-microwells device and (b) real-time polymerase chain reaction (RT-PCR) amplification curves [Color figure can be viewed at wileyonlinelibrary.com]

100 copies/μl of HBV clone were then fluidically distributed into each well of EW-chip by EWOD by applying 40 V between the top ITO electrode and the bottom substrate (for more details see Section 2). The sample was uniformly distributed on each well and the thermal cycling for PCR launched. The results are illustrated in Figure 5. Figure 5a shows the fluorescence image of EW-chip at the end of the amplification processes. The six dark wells (1–5, 3–5, 5–5, 7–5, 9–5, and 11–5) are the negative amplification tests (without primers reagents into these wells), included for the assessment of possible cross-contamination. The image qualitatively shows the level of fluorescence quite uniform in all microwells apart those of negative test as expected in the absence of fluidic cross-contamination.

The quantitative kinetic amplification curves are reported in Figure 5b. Consistently with the qualitative appearing the fluorescence image, the amplification processes occurred consistently in all microchambers containing the PCR primers for the amplification. Actually, the Ct values are 22.8 ± 2 with a coefficient variation of about 8.7%. This indicates a very uniform amplification over all the microwells. On the contrary, the microwells that does not contain the PCR primers for the amplification (negative tests) show a flat signal indicating no amplification occurring. This undoubtedly proves the absence of fluidic cross-contamination.

4 | CONCLUSIONS

In this study, we have described innovative silicon composed of 96 microchamber (200 nl) fluidically actuated through EWOD process for multiparallel detection of nucleic acids. Effect of surface properties on EWOD electroloading was studied to guarantee both the effective EWOD actuation and the biocompatibility versus the PCR reaction. The nucleic acids sensing ability of this platform was successfully proven by real-time PCR experiments using as a model HBV genome target performed with reagent-on-board. Results show very uniform amplification over the 96 microchamber without any cross-contamination process. These features make this system a very appealing potential solution for point-of-care applications.

ACKNOWLEDGMENT

This study was supported by MIUR by means of the national Program PON R&C 20072007–2013,–2013, project "Hyppocrates—Sviluppo di Micro e Nano-Tecnologie e Sistemi Avanzati per la Salute dell'uomo" (PON02 00355).

CONFLICT OF INTERESTS

The authors declare that there are no conflict of interests.

ORCID

Sabrina Conoci http://orcid.org/0000-0002-5874-7284

REFERENCES

Battaglia, S., Petralia, S., Vicario, N., Cirillo, D., & Conoci, S. (2019). An innovative silicon-chip for sensitive real time PCR improvement in pathogens detection. *Analyst*, *Advanced article*, *144*, 2353–2358. https://doi.org/10.1039/C9AN00006B

Berge, B., & Peseux, J. (2000). Variable focal lens con-trolled by an external voltage: An application of electrowetting. *European Physical Journal E*, *3*, 159–163. https://doi.org/10.1007/s101890070029.

Callari, F. L., Petralia, S., Conoci, S., & Sortino, S. (2008). Light-triggered DNA release by dynamic monolayer films. *New Journal of Chemistry*, *32*, 1899. https://doi.org/10.1039/b808118b

Casilli, S., Malitesta, C., Conoci, S., Petralia, S., Sortino, S., & Valli, L. (2004). Piezoelectric sensor functionalised by a self-assembled bipyridinium derivative: Characterisation and preliminary applications in the detection of heavy metal ions. *Biosensors and Bioelectronics*, *20*, 1190–1195. https://doi.org/10.1016/j.bios.2004.04.028

Chun, K., Syndergaard, C., Damas, C., Trubey, R., Mukindaraj, A., Qian, S., … Niemz (2015). A sepsis pathogen identification. *Journal of Laboratory Automation*, *20*, 539–561. https://doi.org/10.1177/2211068214567345

Giancane, G., Borovkov, V., Inoue, Y., Conoci, S., & Valli, L. (2013). Syn-anti conformation switching of a bis-porphyrin derivative at the air-water interface and in the solid state as an effective tool for chemical sensing. *Soft Matter*, *9*(7), 2302 2307. https://doi.org/10.1039/c2sm27141a

Hayes, R. A., & Feenstra, B. J. (2003). Video-speed electronic paper based on electrowetting. *Nature*, *425*, 383–385. https://doi.org/10.1038/nature01988

He, M., & Herr, A. (2010). Automated microfluidic protein immunoblotting. *Nature Protocols*, *5*, 1844–1856. https://doi.org/10.1038/nprot.2010.142

Italiano, F., Buccolieri, A., Giotta, L., Agostiano, A., Valli, L., Milano, F., & Trotta, M. (2009). Response of the carotenoidless mutant Rhodobacter sphaeroides growing cells to cobalt and nickel exposure. *International Biodeterioration & Biodegradation*, *63*, 948–957. https://doi.org/10.1016/j.ibiod.2009.05.001

Jang, J. S., Simon, V. A., Feddersen, R. M., Rakhshan, F., Schultz, D. A., Zschunke, Mi. A., … Jen, J. (2011). Quantitative miRNA expression analysis using fluidigm microfluidics dynamic arrays. *BMC Genomics*, *12*, 144. https://doi.org/10.1186/1471-2164-12-144

Libertino, S., Conoci, S., Scandurra, A., & Spinella, C. (2013). Biosensor integration on Si-based devices: Feasibility studies and examples. *Sensors and Actuators, B: Chemical*, *179*, 240–251. https://doi.org/10.1016/j.snb.2012.09.108

Liu, W., Das, J., Mepham, A. H., Nemr, C. R., Sargentd, E. H., & Kelley, S. O. (2018). A fully-integrated and automated testing device for PCR-free viral nucleic acid detection in whole blood. *Lab on a Chip*, *18*, 1928–1935. https://doi.org/10.1039/C8LC00371H

Mark, D., Haeberle, S., Roth, G., von Stettenz, F., & Zengerlez, R. (2010). Microfluidic lab-on-a-chip platforms: Requirements, characteristics and applications. *Chemical Society Reviews*, *39*, 1153–1182. https://doi.org/10.1039/B820557B

Marziliano, N., Notarangelo, M. F., Cereda, M., Caporale, V., Coppini, L., & Demola, M. A., et al. (2015). Rapid and portable, lab-on-chip, point-of-care genotyping for evaluating clopidogrel metabolism. *Clinica Chimica Acta*, *451*, 240–246. https://doi.org/10.1016/j.cca.2015.10.003

Mugele, F., & Baret, J. C. (2005). Electrowetting: From basics to applications. *Journal of Physics: Condensed Matter*, *17*, 705–R774. https://doi.org/10.1088/0953-8984/17/28/R01

Nelson, W. C., & Kim, C. J. (2012). Droplet actuation by electrowetting-on-dielectric (EWOD): A review. *Journal of Adhesion Science and Technology*, *26*, 1747–1771. https://doi.org/10.1163/156856111X599562

Petralia, S., Alessi, E., & Ventimiglia, G. (2012). Stability evaluation of protein coating for sensing: An application to silicon based lab-on-chip device. *Sensors and Transducers*, *137*, 215.

Petralia, S., Castagna, M. E., Motta, D., & Conoci, S. (2016). Miniaturized electrically actuated microfluidic system for biosensor applications. *BioNanoScience*, *6*, 139–145. https://doi.org/10.1007/s12668-016-0204-2

Petralia, S., & Conoci, S. (2017). PCR technologies for point of care testing: Progress and perspectives. *ACS Sensors*, *2*, 876–891. https://doi.org/10.1021/acssensors.7b00299

Petralia, S., Sciuto, E. L., & Conoci, S. (2017). A novel miniaturized biofilter based on silicon micropillars for nucleic acid extraction. *Analyst*, *142*, 140–146. https://doi.org/10.1039/c6an02049f

Petralia, S., Sciuto, E. L., Di Pietro, M. L., Zimbone, M., Grimaldi, M. G., & Conoci, S. (2017). An innovative chemical strategy for PCR-free genetic detection of pathogens by an integrated electrochemical biosensor. *Analyst*, *142*, 2090–2093. https://doi.org/10.1039/c7an00202e

Petralia, S., Ventimiglia, G., Ceschia, S., Gasparin, M., & Verardo, R. (2017). A novel silver coating for antigen-microarray preparation suitable for application on antibody recognition. *BioNanoSci*, *7*, 449–455. https://doi.org/10.1007/s12668-017-0398-y

Pollack, M. G., Fair, R. B., & Shenderov, A. D. (2000). Electrowetting-based actuation of liquid droplets for microfluidic applications. *Applied Physics Letters*, *77*, 1725–1726. https://doi.org/10.1063/1.1308534

Poltronieri, P., Mezzolla, V., Primiceri, E., & Maruccio, G. (2014). Biosensors for the detection of food pathogens. *Foods*, *3*, 511–526. https://doi.org/.org/10.3390/foods3030511

Rella, R., Siciliano, P., Quaranta, F., Primo, T., Valli, L., Schenetti, L., … Iarossi, D. (2000). Gas sensing measurements and analysis of the optical properties of poly[3-(butylthio)thiophene] Langmuir–Blodgett films. *Sensors and Cactuatros B—Chemical*, *68*, 203–209. https://doi.org/10.1016/S0925-4005(00)00430-5

Sondag-Huethorst, J. A. M., & Fokkink, L. G. J. (1994a). Electrical double layers on thiol-modified polycrystalline gold electrodes. *Journal of Electroanalytical Chemistry*, *367*, 49–57. https://doi.org/10.1016/0022-0728(93)03006-B

Sondag-Huethorst, J. A. M., & Fokkink, L. G. J. (1994b). Potential-dependent wetting of electroactive ferrocene-terminated alkanethiolate monolayers on gold. *Langmuir*, *10*, 4380–4387. https://doi.org/10.1021/la00023a074

Sortino, S., Petralia, S., Condorelli, G. G., Conoci, S., & Condorelli, G. (2003). Novel photoactive self-assembled monolayer for immobilization and cleavage of DNA. *Langmuir*, *19*, 536–539. https://doi.org/10.1021/la0264365

Trantidou, T., Elani, Y., Parsons, E., & Ces, O. (2017). Hydrophilic surface modification of PDMS for droplet microfluidics using a simple, quick, and robust method via PVA deposition. *Microsystems & Nanoengineering*, *3*, 16091. https://doi.org/10.1038/micronano.2016.91

Zhao, C., Ge, Z., & Yang, C. (2017). Microfluidic techniques for analytes concentration. *Micromachines*, *8*, 28. https://doi.org/10.3390/mi8010028

Zhao, Y.-P., & Wang, Y. (2013). Recent advances in gecko adhesion and friction mechanisms and development of gecko-inspired dry adhesive surfaces. *Reviews of Adhesion and Adhesives*, *1*, 114–129. https://doi.org/10.1007/s40544-013-0011-5

SUPPORTING INFORMATION

Additional supporting information may be found online in the Supporting Information section at the end of the article.

How to cite this article: Petralia S, Motta D, and Conoci S. EWOD silicon biosensor for multiple nucleic acids analysis. *Biotechnology and Bioengineering*. 2019;1–8. https://doi.org/10.1002/bit.26987